Extending holographic LEED to ordered small-unit-cell superstructures

K. Reuter,* J. A. Vamvakas, and D. K. Saldin
Department of Physics and Laboratory for Surface Studies, University of Wisconsin-Milwaukee, P.O. Box 413, Milwaukee, Wisconsin 53201

V. Blum, M. Ott, H. Wedler, R. Döll, and K. Heinz
Lehrstuhl für Festkörperphysik, Universität Erlangen-Nürnberg, Staudtstrasse 7, D-91058 Erlangen, Germany
(Received 19 December 1997)

Following on the success of the recent application of holographic LEED to the determination of the three-dimensional atomic geometry of Si adatoms on a SiC(111)$p(3\times3)$ surface, which enabled that structure to be solved, we show in this paper that a similar technique allows the direct recovery of the local geometry of adsorbates forming superstructures as small as $p(2\times2)$, even in the presence of a local substrate reconstruction. [S0163-1829(98)07928-4]

I. INTRODUCTION

The short inelastic scattering length of low-energy electrons makes them ideal tools for surface crystallography. The energy variations of the intensities [$I(V)$ curves] of the reflected Bragg beams depend sensitively on the structure of the few outermost atomic layers, which is usually deduced by a trial-and-error fitting to simulated $I(V)$ curves from model structures.[1]

Even for a single model structure the calculation of a set of $I(V)$ curves is no trivial task. The calculation requires two main ingredients: first, a representation of the scattering properties of each of the atoms of the presumed structure—this is parametrized in a set of energy-dependent *phase shifts* for each angular momentum quantum number. Second, it is necessary to evaluate the scattering of electrons among all atoms of the sample. During the 1960's and 1970's many ingenious methods were developed to efficiently sum the multiple-scattering paths followed by the electrons from source to detector.[1,2]

Although many of the simpler surface structures were solved during this period, it was also becoming clear that more complicated structures would probably forever lie beyond the reach of standard multiple-scattering trial-and-error fitting methods due to the exponential scaling of computer time with the number of parameters to be fitted. A simple example makes this abundantly clear: suppose we need to determine the three Cartesian coordinates of N symmetry inequivalent atoms, and for this purpose we consider models with 10 values of each coordinate. The time required for an exhaustive search among these parameters is $T=S\times10^{3N}$, where S is the time required to calculate the low-energy electron diffraction (LEED) spectra from each model. Taking $S=1$ second and $N=3$ we find $T=30$ years. Just doubling the number of atoms to $N=6$ results in a time T of the order of the age of the universe! In the latter case, increases in computer speeds by even a millionfold would only bring T down to a few millennia. (Of course, the above time estimates would be reduced considerably if it were judged that not all three Cartesian coordinates need to be determined independently.)

Obviously there is a need to examine some alternatives to exhaustive trial-and-error searches. Consequently, procedures applying a directed search in the multidimensional parameter space have been developed (for reviews see, e.g., Refs. 3 and 4). In this context the testing of simulated annealinglike and genetic algorithms[5] are certainly steps in a most promising direction. Also, quasidirect methods were developed allowing a search-free optimization of structural parameters once a model near the correct structure had been found or guessed.[6] The other approach that has shown considerable promise for LEED in recent years has been the holographic method.[7]

This has been applied primarily to surfaces containing adatoms of either the same or different species than the surface atoms. Initially it was used to reconstruct a three-dimensional (3D) image of the local geometry of disordered atomic adsorbates on a surface from the *diffuse* LEED (DLEED) patterns in which the electron intensity between the Bragg spots is capable of a holographic interpretation.[8] Recent work has shown that essentially the same numerical algorithm is able to form an image of the local geometry of Si on a SiC(111)-$p(3\times3)$ surface.[9] This work was important in that it showed that the holographic method can be applied to the case of an ordered array of adatoms on a surface by operating on the intensities of superstructure (or fractional-order) Bragg spots, and in that it actually was the catalyst to the solution of this rather complex structure that was most likely beyond the scope of the current techniques of conventional LEED analysis.

As has been pointed out earlier,[10–13] a set of superstructure Bragg spots from an ordered array of adsorbates may be thought of as sampling the corresponding diffuse LEED intensities at the positions of these spots. In the case of a large adsorbate unit cell like the (3×3) one in the above-cited case, the diffuse intensities may be thought as being sampled over a rather dense grid in the reciprocal-space planes parallel to the surface. However, within the class of ordered adsorbate superstructures, those of smaller unit cells are much more frequently observed. One such set of superstructures that still can present difficulties for present state-of-the-art conventional LEED methods are the $p(2\times2)$ structures. It is

the aim of the present paper to show that even this class of adsorbate superstructures may also be brought within the purview of holographic LEED methods.

II. THE ''CORRECT'' ALGORITHM FOR DIFFUSE LEED

Holographic methods have already been employed successfully to reconstruct the local geometry of disordered atomic adsorbates on a crystal surface.[14–17] In the corresponding diffuse LEED patterns, diffraction intensity can be measured in the areas between the Bragg spots. This intensity arises from elastic scattering from a surface exhibiting structural elements lacking lateral translational symmetry. If one considers elastic scattering from a surface containing a single adsorbate atom, it is obvious that the DLEED intensity H_a it gives rise to can arise from just those scattering paths that include a scattering from the adsorbate atom since this is the only one that breaks the lateral periodicity of the surface. The diffuse intensity from a disordered layer of such adsorbates in the same local sites of a flat substrate may be written[18]

$$H(\mathbf{k}) = H_a(\mathbf{k}) S(\mathbf{k}_\parallel), \tag{2.1}$$

where $\mathbf{k} \equiv (\mathbf{k}_\parallel, k_\perp)$ is the wave vector of the detected electron, $\mathbf{k}_\parallel$ its component parallel to, $k_\perp$ that perpendicular to the surface, and S is a lattice factor that quantifies the degree of long-range order among the adsorbates. In the case of perfect lattice-gas disorder, which might be expected at very low adsorbate coverages, S becomes constant and equal to N, the total number of adsorbates illuminated by the electron beam, except in the parts of the diffraction pattern occupied by the substrate Bragg spots (which are excluded in practice), where it is equal to N^2. Thus the accessible part of the DLEED pattern is just a more intense version of H_a.

The holographic view of DLEED (Ref. 8) focuses on the fact that the obligatory scattering at an adsorbate leads to a natural separation of all scattering paths: electrons the final scattering of which is by an adsorbate form the *reference* wave $R(\mathbf{k})$, while those scattered subsequently by substrate atoms before reaching the detector provide the *object* wave $O(\mathbf{k})$. On this picture of the adsorbate as a microscopic beam splitter, H_a can be written

$$H_a(\mathbf{k}) = |R(\mathbf{k}) + O(\mathbf{k})|^2. \tag{2.2}$$

For a single DLEED pattern, it was suggested that the holographic reconstruction algorithm derived by Barton[19] for photoelectron holography could be used to produce a 3D image of the local atomic environment of the adsorbate. Consequently, the numerical inversion algorithm can be formulated as a phased 2D Fourier transform of the DLEED data over $\mathbf{k}_\parallel$.

Due to the fact that DLEED patterns of different electron energies can be measured easily, the idea emerged that information from several such patterns could profitably be combined in reconstructing the image.[8] Indeed, multienergy reconstruction algorithms[20,22] led to a considerable improvement in the images that could at that time be called reliable for the first time. Apart from suppressing the unwanted holographic twin image, the additional stationary-phase condition arising from the integral over energies was designed to single out the contributions due to the kinematic object wave. A benefit from this is that corrections for the remaining anisotropies of the reference and object waves may then be performed by assuming rather simple forms for these quantities.[21] Subsequently, many variants of multienergy reconstruction algorithms have been suggested.[23]

The most successful of such holographic DLEED inversion algorithms to date has been the *Compensated Object- and Reference-wave Reconstruction by an Energy-dependent Cartesian Transform* (CORRECT).[24] Unlike previous multienergy algorithms that perform the 3D holographic reconstruction integral in a polar coordinate system (angle and energy), this transform operates on a Cartesian data input $(\mathbf{k}_\parallel, k_\perp)$.[17] Considering that a superstructure spot is characterized by a constant $\mathbf{k}_\parallel$ under changes of electron energy, this algorithm has the advantage of being most suitable for an extension to diffraction data from ordered superstructures. With this algorithm, the reconstructed real-space distribution around the adsorbate $|B(\mathbf{r})|^2$ [where $\mathbf{r} \equiv (\mathbf{r}_\parallel, z)$ is a position vector relative to an origin at an adsorbate with components $\mathbf{r}_\parallel$ parallel and z perpendicular to the surface] can be calculated via

$$B(\mathbf{r}) = \int \int_{\mathbf{k}_\parallel} \left[\int_{k_\perp} K(\mathbf{k}_\parallel, k_\perp; \mathbf{r}) \chi(\mathbf{k}_\parallel, k_\perp) e^{-i(kr - k_\perp z)} dk_\perp \right] \times e^{i \mathbf{k}_\parallel \cdot \mathbf{r}_\parallel} d^2 \mathbf{k}_\parallel . \tag{2.3}$$

Apart from the obvious fact that this involves a 3D integral over reciprocal space, two noteworthy features are: first, that it operates not directly on the measured intensities H, but rather on a contrast-enhancing and normalizing function

$$\chi(\mathbf{k}_\parallel, k_\perp) = \frac{H(\mathbf{k}_\parallel, k_\perp) - H_{av}(\mathbf{k}_\parallel)}{H_{av}(\mathbf{k}_\parallel)} \tag{2.4}$$

with

$$H_{av}(\mathbf{k}_\parallel) = \frac{\int H(\mathbf{k}_\parallel, k_\perp) dk_\perp}{\int dk_\perp}. \tag{2.5}$$

It has been shown theoretically[24] that the use of such a χ function helps to partially remove the self-interference terms $|R(\mathbf{k})|^2$ and $|O(\mathbf{k})|^2$ in the DLEED intensity in Eq. (2.2), which give rise to high intensities around the origin of the reconstructed real space distribution. More importantly, χ has been designed to remove effects due to partial ordering among the adsorbates. Since for flat substrates (i.e., those not exhibiting steps) the lattice factor S in Eq. (2.1) is an exclusive function of $\mathbf{k}_\parallel$, it is unaffected by the integrals over $k_\perp$ in the definition of χ and hence cancels out. Deviations from perfect lattice-gas disorder at higher coverages, which give rise to modulations of S, can thus be efficiently suppressed.[17]

The anisotropic scattering of low energy electrons by the adsorbate beam splitter makes the local environment of the adsorbate show up only within the forward-scattering cone of the incident wave when images are reconstructed by previous inversion algorithms.[25] Full 3D images are only formed with such algorithms by taking sets of DLEED data of different electron energies for each of a number (at least two) of different directions of incident electrons.[14,15] Of course, this causes considerable experimental effort and so it

would be preferable to use a set of DLEED patterns from just the most reliably-measured normal incidence data, which allow us to improve the data quality by off-line averaging according to the underlying surface symmetry. This becomes possible with the use of the CORRECT algorithm, due to its compensation for the anisotropy of the reference wave by estimating its value at the position of a scatterer, by inclusion of the kernel

$$K(\mathbf{k}_{\parallel},k_{\perp};\mathbf{r})=\left[\frac{f_a(\mathbf{k}_i\cdot\hat{\mathbf{r}})+C}{r}\right]^{-1}. \tag{2.6}$$

under the integral in Eq. (2.3). Here $f_a(\mathbf{k}_i\cdot\hat{\mathbf{r}})$ is the atomic scattering factor of the adsorbate, $\hat{\mathbf{k}}_i$ is the direction of electron incidence, and C is the so called kernel constant (which we take to be real, and which represents a zeroth-order approximation to the backscattering by the substrate prior to scattering by the adsorbate). An order of magnitude estimate can be made for C from its theoretical derivation (leading to $C_{\mathrm{ONi}}\simeq 0.75$ Å and $C_{\mathrm{KNi}}\simeq 2.20$ Å for both of the systems, O/Ni and K/Ni, treated in this paper).[24] In general, the effect of C is well defined and hence its value can also simply be optimized, such that all atoms in the local adsorption geometry show up with similar brightness.[26]

This algorithm has been shown to give reliable images using theoretical,[24,26] as well as experimental, DLEED data.[16,17]

III. DLEED AND LEED INTENSITIES

Even though research on surfaces giving rise to diffuse LEED intensities can provide important information on initial (disordered) stages of adsorption, the great majority of structures investigated manifest long-range order in the plane parallel to the surface (henceforth referred to as the *lateral* plane). Particularly, many systems, where this order results in the surface having larger lateral unit cells than that of the bulk, put rather heavy demands on the standard quantitative LEED analysis. The large number of structural parameters to be determined increases exponentially the number of trial structures to be considered. For such structures, the lattice factor S becomes a sum of δ functions with peaks at the reciprocal lattice rods due to the period of the new superstructure. In other words, destructive interference between the waves originating from different adsorbate-substrate clusters extinguishes all diffraction intensity but that concentrating in the newly formed, sharp superstructure spots.

Nevertheless, these superstructure spots have been proven to contain the same crystallographic information on the local environment of the adsorbate: as long as scattering between different adsorbates can be neglected, the diffuse intensity from an adsorbate and its local surroundings corresponding to a particular value of $\mathbf{k}_{\parallel}$ has the same energy dependence as the superstructure spot intensity from an ordered array of such adsorbates in an equivalent local adsorption geometry[10] and of a surface reciprocal lattice vector equal to the same value of $\mathbf{k}_{\parallel}$. As pointed out earlier,[11] the superstructure spots may be thought of as sampling the DLEED intensity distribution of the corresponding lattice gas on a finite grid. It was also shown that the neglect of intra-adsorbate scattering holds even for relatively dense superstructures under normal electron incidence.[11]

With this understanding, a DLEED holographic inversion algorithm like CORRECT may, in principle, be applied to superstructure spot intensities—in particular, since the latter takes its input diffraction intensities on a Cartesian grid in reciprocal space. The only apparent difference is that the finite sampling breaks down the integral over $\mathbf{k}_{\parallel}$ to a discrete sum. However, a numerical implementation of the reconstruction algorithm does this even in DLEED, so that the real difference is the strongly *reduced* data resolution in $\mathbf{k}_{\parallel}$.[26] In this respect, the larger the new surface period, the more fractional-order spots and hence the more data left for the algorithm and the more similar the situation becomes to the former DLEED case. Recently, the CORRECT algorithm was thus successfully applied to the $p(3\times 3)$ reconstruction of SiC(111).[9] The high density of superstructure spots corresponding to such a large reconstructed surface unit cell allowed the application of the DLEED algorithm without any modifications caused by the finite sampling. Differences that appear for small ordered superstructures with their even further restricted database will be addressed in the next section.

Note that the application to SiC(111) highlights the fact that, for ordered superstructures, it becomes irrelevant for holography whether the microscopic beam splitter is an adsorbate on top of a substrate or belongs intrinsically to the substrate itself as in the case of adatoms in surface reconstructions. This increases considerably the number of systems to which holographic LEED may be applied. The main requirements are that the beam-splitter atom is the principal cause of the break of the bulk lateral periodicity and that there be only one such atom per superstructure unit cell (in order to prevent intermixing of images centered on several such holographic reference-wave sources). If large, inequivalent adsorbate overlayer domains exist on the surface the resulting image would be a simple superposition of the local atomic structure around each adsorbate. Since the reconstructed image reveals essentially the local bonding geometry of the adsorbates, even the existence of more than one inequivalent superstructure domain is immaterial, provided the local geometries of the adsorption sites are identical.

As a last point, it is important to mention that for the application to conventional LEED data, the strong reduction in $\mathbf{k}_{\parallel}$ data resolution goes hand in hand with a strong increase in the available energy range and data quality. Conventional LEED spot intensities can be measured up to much higher energies ($\simeq 400-500$ eV and even higher at low temperatures) than DLEED distributions, which suffer from disturbing effects from the much brighter substrate Bragg spots[11] and greater contributions from thermal diffuse scattering at higher energies. Since atomic scattering factors show a much weaker energy dependence at elevated energies, this additionally accessible data range is also particularly favorable for any holographic inversion algorithm, which tends to rely on rather smoothly varying electron scattering properties. Further, the signal-to-noise ratio of the bright discrete spots is much higher than that of diffuse intensities, and contributions from thermal diffuse scattering are less important and easier to subtract. In conclusion, the data acquisition of discrete LEED diffraction spots is thus much more standard and reliable than that of diffuse LEED distributions. Conse-

quently, the extension of holographic inversion algorithms to ordered systems will make this technique much more applicable to a wider range of systems.

IV. LIMITS OF VALIDITY FOR SMALL SUPERSTRUCTURES

Even though the above-mentioned application to SiC(111)-$p(3\times3)$ employed the unmodified CORRECT algorithm, it can only be seen as an intermediary step towards the real extension of DLEED holography to ordered superstructures. There are very few such large-unit-cell reconstructions with the additional requirement of having only one prominent atom to serve as a holographic beam splitter. In general, surface structures will show smaller periodicities with even less fractional-order spots remaining for the inversion algorithm. In this case, the coarse sampling must evidently result in perturbing effects on the integral transform designed for continuous data distributions. Hence, there are two questions to be addressed: (i) Will there be restrictions on the general validity of the method? (ii) Is there a way to make more efficient use of the smaller quantity of the remaining data? We will treat question (i) first and defer question (ii) to the next section.

When considering restrictions on the general validity, the key point to notice is that the primary consequence of the prevailing surface periodicity is to reduce the continuous $\mathbf{k}_\parallel$ integral in Eq. (2.3) to a discrete sum. Since the term inside the square brackets in Eq. (2.3) is a slowly varying function of $\mathbf{r}$, this two-dimensional integral is essentially a Fourier transform in $\mathbf{k}_\parallel$. The problem encountered here is hence similar to the well-known numerical problem of discrete Fourier transforms. The sampling theorem[27] states in this case, that when a function that is not bandwidth limited is sampled on discrete intervals of magnitude Δ, there will be a frequency range in the dual space limited by the *Nyquist* frequency f_c:[28]

$$[-f_c;f_c] \quad \text{with} \quad f_c=\frac{2\pi}{2\Delta}. \tag{4.1}$$

All power spectral densities of the original function that would lie outside of this range will be spuriously moved inside by *aliasing*, and the Fourier transform will be periodic due to aliasing of the spectral density outside of f_c.

For the application of this theorem to our present problem, consider for simplicity a laterally one-dimensional example with a surface reconstruction with a period of n times the bulk one. This gives rise to $(n-1)$ fractional order diffraction spots per Brillouin zone in the LEED pattern. The sampling interval Δ will thus be g/n, where g is the magnitude of the reciprocal lattice vector corresponding to the lateral bulk periodicity given by

$$g=\frac{2\pi}{a_p} \tag{4.2}$$

and a_p the lateral lattice constant. Substitution in Eq. (4.1) determines the *Nyquist* critical frequency to be

$$f_c=\frac{na_p}{2}. \tag{4.3}$$

Let us think of some hypothetical superstructure periodicities: $n=1$ represents same periodicity of bulk and surface, and hence results in no fractional-order spots. Our holographic method is not applicable here. On the other hand, $n>2$ leads to a larger number of fractional-order spots and a larger usable data density. Any restrictions on the algorithm's validity will be expected to affect such a case little, and one can argue that it suffices to derive such limits for the worst case, namely $n=2$.

From Eq. (4.3) above, $f_c=a_p$ for this case. However, so far we have neglected the fact that the integer-order spots have to be excluded from the inversion algorithm since they are dominated by pure substrate scattering paths. This will double the effective sampling interval Δ to g and consequently halve the critical frequency to $a_p/2$. On the other hand, for real laterally two-dimensional cases, the effective sampling interval may also lie between these two estimates, depending on the periodicity in the other lateral direction. For example, consider the LEED pattern from a $p(2\times2)$ superstructure: there will be rows of superstructure Bragg spots in the direction of each reciprocal lattice vector at intervals of $g/2$ and alternate rows that include integer-order spots where the superstructure spots are found at intervals of g. *Cum grano salis* we may therefore argue, that the critical frequency for this case must lie somewhere in the range

$$\frac{a_p}{2}<f_c<a_p. \tag{4.4}$$

The sampling theorem now implies that any real-space intensity represented by the function $|B(\mathbf{r})|^2$ in Eq. (2.3) that would normally appear outside a lateral range of $\pm f_c$, is moved inside by aliasing. A natural consequence would be severe image distortions due to these contributions. Fortunately, the algorithm is saved by the heavy damping of the low energy electrons inside the crystal, which reduces strongly any contribution to the diffraction intensity from atoms farther from the adsorbate. Also, holographic fringes due to more distant atoms will be of higher frequency in reciprocal space that may be beyond the available data resolution. Thus we may deduce that any such aliased contributions inside the critical frequency range $\pm f_c$ be small compared to the real intensities corresponding to true atomic positions [in Fourier transform terms this can be rephrased that $H(\mathbf{k})$ is bandwidth limited]. This reasoning is corroborated by the fact that, in all previous investigations using DLEED data, where no such aliasing effects are expected, the only atomic positions recovered belonged to the direct local adsorption geometry and no intensity due to further outlying atoms appeared in the reconstructed images.[16,17,24,26]

The more important consequence of the sampling theorem in the present case is the folding out of intensity outside of the critical range f_c. In other words, aliasing restricts the range of lateral validity of the algorithm to

$$\frac{a_p}{2}<f_c<a_p \tag{4.5}$$

for $p(2\times2)$ structures. Outside of this range one cannot be sure whether reconstructed intensity is due to real atoms or

solely due to aliased contributions. Note, that even in this worst case, the aliasing does *not* destroy the algorithm's applicability: the latters' main task is to recover atomic positions of the local adsorption geometry, or the local adatom environment. In almost any imaginable case the lateral distance of such neighboring atoms is less than a_p, and hence still accessible to the holographic inversion algorithm. In particular, for the case of a hollow-site adsorption on a fcc(001) surface, which we discuss later, the lateral distance of the four nearest first-layer substrate atoms is $a_p/2$ and thus well within the critical range. Even though the very restricted data resolution will thus not lead to a breakdown of our holographic scheme, we must keep clearly in mind its limited range in the direction parallel to the surface.

V. DROPPING THE χ FUNCTION

We now consider the question whether the limited quantity of remaining data in conventional LEED should be treated differently by a holographic algorithm. After establishing the equivalence, for our purposes, of DLEED and LEED intensities, it is obvious that the general form of the 3D integral transform does not need to be changed, since the algorithm still targets the same scattering-path phases. On the other hand, as mentioned earlier, the primary purpose for the design of the contrast-enhancing χ function in Eq. (2.4) has been to suppress effects of partial ordering among the adsorbates, which leads to modulations in the lattice factor S. However, for the case of an ideally ordered superstructure on a flat surface, S becomes a sum of δ functions with equal value at each of the remaining reciprocal lattice rods. Any filtering effect of χ is thus no longer needed.

The second advantage of presenting data to the inversion algorithm in the form of the χ function has been the partial removal of the self-interference terms in Eq. (2.2), which would be expected to give rise only to low-frequency oscillations in the diffraction pattern. The principal argument for this is that oscillations in $H(\mathbf{k})$ are due mainly to the reference-object interference terms $R^*(\mathbf{k})O(\mathbf{k})$ and $R(\mathbf{k})O^*(\mathbf{k})$ and that hence $H_{av}(\mathbf{k}_\parallel)$ as defined in Eq. (2.5) represents a rough approximation to the remaining self-interference terms in $H(\mathbf{k})$.[24] It is clear that this crude estimate causes a degradation of the input diffraction data in the construction of the χ function. This is of no importance in the DLEED case, where an abundance of data tends to average out such deleterious effects, and allows predominantly the positive consequences of the χ function to be noticed.[17]

With the filtering effect not required for superstructures, and knowing that, due to the limited quantities of available conventional-LEED data, it will be advantageous to use rather the undegraded measured intensities $H(\mathbf{k})$ as input to the reconstruction algorithm, we seek an alternative way to suppress the self-interference contributions to the images. This can actually be achieved with a much simpler procedure: since these terms in the diffraction intensity are primarily of low frequency in the diffraction data, they would be expected to cause distortions mainly in the part of the reconstructed image near its origin.[8,12,19,24] Given that the origin is defined by the position of the atomic beam splitter, no other atoms are expected within a hard-sphere radius of that adatom or adsorbate. We therefore suggest, that ignoring any image features within such a radius [i.e., setting $B(\mathbf{r})$ to zero in that region], is as effective a method of suppressing the self-interference terms as by the use of a χ function, but without the danger of degradation of the useful holographic fringes in the diffraction data.

VI. TEST CASE OF O/Ni(001) *p(2×2)*

With these modifications, our algorithm should be applicable to LEED data from smaller ordered superstructures. Such data are characterized by a lower reciprocal-space density of fractional-order spots, and there may indeed be a lower limit to this density for effective holographic reconstruction. Thus in the order of surface structures, as characterized by overlayer sizes, holographic LEED promises to occupy a niche essentially complementary to that of conventional quantitative LEED methods: the smaller surface unit cells possess a limited number of free structural parameters, and can be almost routinely solved by standard trial-and-error procedures,[4] while the larger superstructures are more problematical due to the exponential scaling with the number of parameters, as discussed earlier. In contrast, the larger density of fractional-order Bragg spots from the larger overlayer unit cells makes their LEED pattterns more favorable for an holographic analysis, as our earlier work on the SiC(111) (3×3) has already demonstrated.[9] In the present paper we show that even superstructures as small as $p(2\times2)$, which have in the past posed considerable difficulties for conventional LEED analysis, may be brought within the purview of the holographic method.

As an initial test system we chose the $p(2\times2)$ phase of O/Ni(001). Because this is an extensively investigated and well-known system, it is appropriate for testing methodologic advances: since Ni is a strong scatterer and O a weak one adsorbed very close to the surface, it can be argued that this structure represents a rather unfavorable scenario for holographic techniques, which rely on dominant scattering by the O atom to enhance the reference wave and a suppression of intra-Ni and O-Ni multiple scattering. A successful recovery of the adsorption site in this case would suggest a general applicability of our method, especially on, e.g., lighter scattering substrates like Si.

VII. IMAGE DISPLAY SCHEME

The reconstructed images in this paper will be displayed in perspective to reveal their full 3D real-space geometry. The function $|B(\mathbf{r})|^2$ is calculated from Eq. (2.3) on a grid of 0.2 Å resolution inside a cylinder of depth 3.5 Å and a lateral radius of 2.0 Å, consistent with our estimate of the limits of lateral validity for the unit-cell parameter $a_p = 2.49$ Å for Ni. All atoms that specify the local adsorption geometry of O/Ni(001)-$p(2\times2)$ are located within this volume and their positions should therefore be retrievable by our method. Small spheres, with diameters proportional to the reconstructed intensity $|B(\mathbf{r})|^2$ and whose gray shading varies from white for the lower intensities to black for the higher ones, are drawn at the grid points. The origin of the coordinate system is defined by the adsorbate (beam splitter), which is artificially added to facilitate the understanding. No intensity is calculated inside a sphere of 1.0 Å around this

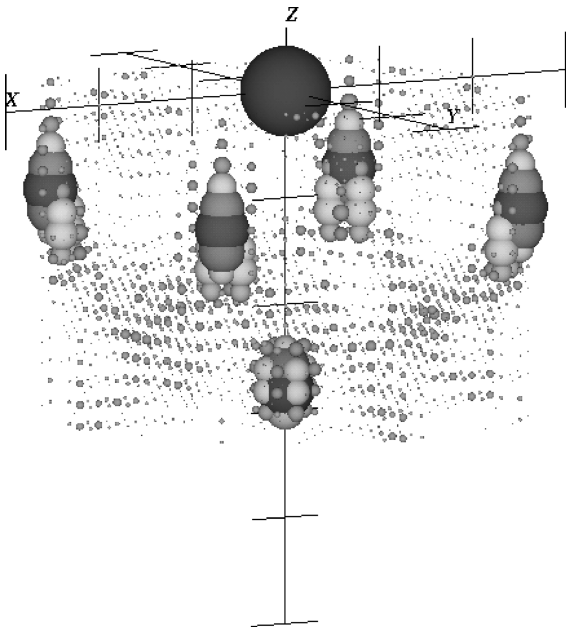

FIG. 1. Recovered local geometry of the O adsorption site from LEED data calculated for a model Ni(001)-$p(2\times2)$ surface with an unreconstructed substrate. The electron energy range of the data used is 130–400 eV, the kernel constant $C=0.70$ Å, and the maximum noise level in the image was found to be 44% of the maxima denoting the atom positions. For details on the display procedure, see Sec. VI.

origin to suppress the self-interference terms as reasoned above.

Even though the commonly used 2D cut planes through a reconstructed image may be more suited for an exact analysis of the atomic positions,[26] we believe that the overall 3D presentation of the reconstruction result not only is more honest (no choice of presentation of ''particular'' cut planes), but also focuses better on the main task of the holographic technique: a direct insight into the essential features of a structure, i.e., in this case the adsorption site.

VIII. SIMULATED DATA FROM UNRECONSTRUCTED SUBSTRATES

As a first step we simulated LEED $I(V)$ data for a simplified O/Ni(001)-$p(2\times2)$ geometry: O residing in the fourfold symmetric hollow site of a bulk-truncated Ni(001) surface at an adsorption height of 0.9 Å.[29] The simulation was carried out with the standard van Hove-Tong computer code[2] using up to 11 phase shifts representing atomic scattering properties (this was found to be appropriate for the envisioned energy range). The data set generated comprises the $I(V)$ curves of all fractional-order spots for the energies 100–400 eV. This represents a typical and experimentally feasible range for LEED investigations. To closely simulate the conditions of a typical LEED experiment, the only data used was that collectible from within a 50° polar semiangle, which corresponds to the standard angular range of conventional electron detectors,[4] and additionally had been shown to be the most appropriate in earlier holographic DLEED investigations.[26]

The reconstructed image shown in Fig. 1 clearly identifies the fourfold adsorption site. An unambiguous distinction between the five atoms of the Ni local adsorption geometry and remaining residual ''noise'' on the image is easily possible. The highest such noise at nonatomic locations is at 44% of the intensity of the identified atoms. The constant C in the integral kernel K of Eq. (2.6) has been optimized to a value of 0.70 Å to give approximately equal intensity for both first- and second-layer atoms.[26] This value agrees very well with the order-of-magnitude estimate derived from theory as described in Sec. II.

The most important property of a direct inversion algorithm when applied to *a priori* unknown systems, is its stability. No fundamentally different information, that could lead to wrong predictions of structural features, should be reconstructed when changing the parameters of the algorithm. With most of the data base parameters dictated by the experiment, the most influential one left to be adjusted is the energy range of the data. Since the effect of the finite energy integral in Eq. (2.3) is only to *suppress*, and not to *erase* multiple scattering contributions, it is to be expected that the image quality can vary as a function of the energy range used. Due to anisotropies in the atomic scattering factors sometimes even smaller ranges may lead to improved images. However, changing the upper and lower energy boundaries should not result in completely different images, on the basis of which wrong adsorption sites would be inferred. We checked this and found the image to be stable when increasing the lower boundary or decreasing the upper one by approximately 60 eV, i.e., the maximum intensities were always found at the site of the five identified atoms. The use of even smaller energy ranges caused the collapse of the algorithm as expressed by very noisy images with many new intensity peaks. So, no false adsorption site could have been obtained from the present data.

The vertical position of all atoms is retrieved to within a 0.2 Å accuracy. As already experienced with DLEED data,[26] the lateral position of the first-layer Ni atoms, which appear only due to the inclusion of the integral kernel K, has a much greater uncertainty of $\simeq0.5$ Å. Also, this lateral position can shift inwards or outwards (see results in the next section) depending on the exact scattering geometry. This effect has to be related to the simplicity of the compensating kernel, which at its present stage includes only a zeroth-order approximation to the backscattering properties of the system[24] and is hence very sensitive to details of the atomic scattering factors. However, the unambiguous recovery of the essential features of a structure (like the adsorption site), is more than sufficient to allow a subsequent refinement by the conventional quantitative LEED analysis.

To verify the generality of the result obtained, we simulated a second data set, with a different adsorbed chemical species and adsorption height, but with all other parameters unchanged. Consistent with the determination of the related K/Ni(001)-$c(4\times2)$ structure,[30] we positioned K in the fourfold hollow site with an adsorption height of 2.56 Å in a hypothetical $p(2\times2)$ arrangement. Figure 2 shows that this adsorption geometry is reconstructed with quality and clarity comparable to that in the case of O/Ni. The optimized kernel constant $C=2.35$ Å again corresponds very well to its theoretical estimate. The slightly higher noise level of 63% is probably related to the K scattering factor, but nevertheless

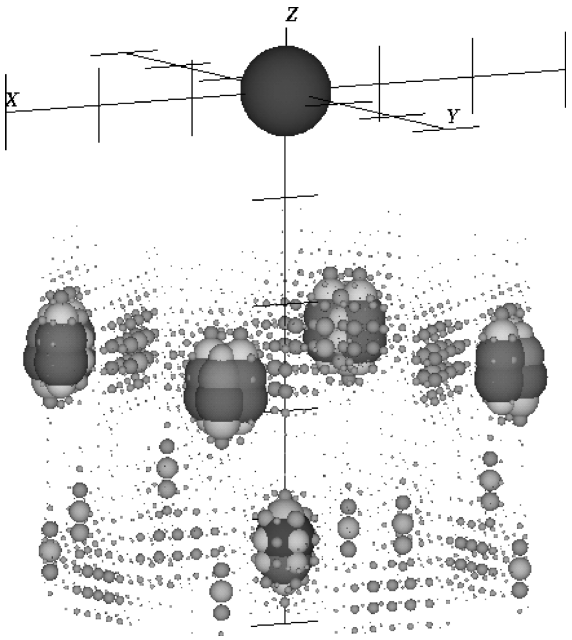

FIG. 2. Same as Fig. 1, except for a model K/Ni(001)-$p(2\times2)$ structure. The electron energy range was 160–385 eV, the kernel constant $C=2.35$ Å and the maximum noise level at 63% of the maxima at the atom positions.

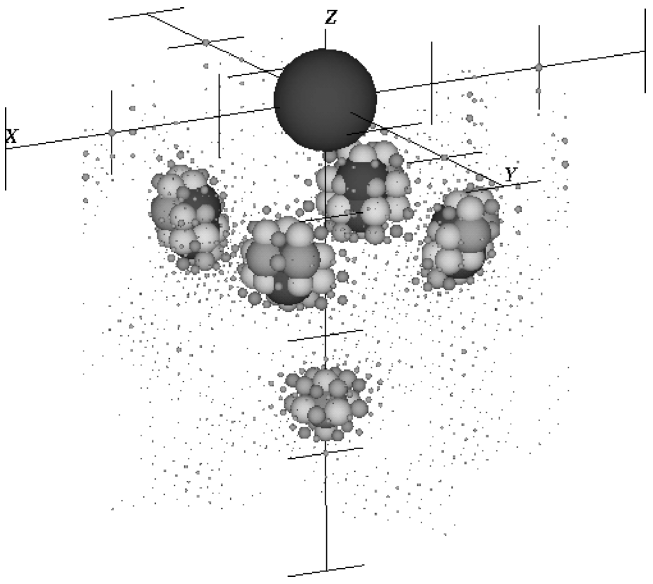

FIG. 3. Same as Fig. 1, except that the LEED data is calculated from a model that had been fitted to experimental LEED data in a previous quantitative LEED study. This model includes reconstruction of the substrate and fitted thermal vibration parameters. The electron energy range used was 112.5–362.5 eV, the kernel constant $C=0.95$ Å and maximum noise level found to be 37% of the maxima at the atoms.

allows an unambiguous identification of all 5 atoms.[31] The new vertical positions due to the enlarged adsorption height are again correct within 0.2 Å and the lateral shift of the first-layer atoms is comparable to the previous case.

The stability encountered with respect to changes of the energy range used is even increased with respect to O/Ni (variations of up to 90 eV are possible), which corroborates our hypothesis of O/Ni as an unfavorable system for holography: the smaller multiple K-Ni scattering due to the increased adsorption height, together with the stronger reference wave due to the K, reduce the required minimum-energy range for multiple-scattering suppression. Consequently, we are led to believe that the two results presented here suggest the general applicability of the modified CORRECT algorithm.

IX. REALISTIC SIMULATION FROM RECONSTRUCTED SUBSTRATES

A typical concern often raised about results of the type presented in the last section is that such simplified simulations cannot be compared to real data as obtained from any realistic structure. Since the van Hove-Tong computer code takes proper account of all multiple scattering, the main difference between data as in the last section and theoretical data as used for actual quantitative LEED analyses consists of two points: thermal vibrations and structural deviations from bulklike truncation such as, e.g., layer relaxations or buckling. It is then argued that both effects might possibly influence the holographic algorithm.

In order to address this question, we simulated a data set, where all structural and nonstructural parameters involved in the dynamical LEED calculation were taken exactly as they had been obtained in the previous quantitative analysis of the O/Ni(001)-$p(2\times2)$ system.[29] Coincidentally, our previous test system proved again to be a rather unfavorable one with respect to both of the above-mentioned features: not only is the determined vibrational amplitude of the O of 0.3 Å unusually high, but also the Ni substrate experiences relaxations of the first two layer spacings ($d_{12}=1.80$ Å and $d_{23}=1.75$ Å), and a relatively strong buckling of 0.10 Å in the second layer. In common with the previous simulations, the full data set comprised again of all fractional-order spots in the energy range 100–400 eV and the holographic reconstruction was carried out by exactly the same procedure as described in the last section.

Consequently, the result shown in Fig. 3 is particularly gratifying. The local adsorption geometry is recovered just as clearly as from the simplified data. Stability with respect to changes of the energy range used and the accuracy of the recovered atomic positions are found to match very well with the ones described in the preceding section. Note, however, that the unstable lateral position of the first-layer atoms now appears shifted inward from the correct value as had already been pointed out in the last section. Interestingly, the overall noise level in the image is, at 37%, even slightly lower for this ''tougher'' more realistic model. Knowing that thermal vibrations lead to a reduction of the effective electron coherence length, it might actually be argued that this effect helps reduce disturbing multiple-scattering contributions due to atoms further from the adsorbate and hence benefits a holographic inversion.

However, the theoretical objection concerning structural deviations from bulklike positions has to be taken more seriously. Any substrate atom whose position deviates from that expected from its ideal lattice position, such as the buckled second-layer Ni atom, could, in principle, act as another conduit for electrons to the fractional-order Bragg spots. The standard argument for neglecting these contributions in the

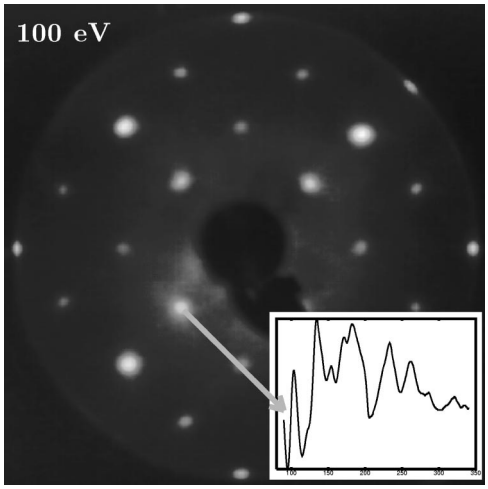

FIG. 4. Experimental LEED pattern from a O/Ni(001)-$p(2\times2)$ surface for an electron energy of 100 eV. The inset shows the $I(V)$ curve of the $(\frac{1}{2}\ 0)$ beam.

holographic theory has been that atoms that only differ slightly from their lattice positions contribute rather weakly to the resulting diffraction intensity, in comparison to the major rupture of the periodicity due to the introduction of a new atom, such as an adsorbate or adatom. As a further theoretical test, we repeated the simulation for the realistic O/Ni(001)-$p(2\times2)$ geometry, but this time with the second-layer buckling artificially doubled to 0.2 Å. Even for this case, the complete adsorption geometry was again retrievable under otherwise identical parameters. The only apparent effect of the increased buckling amplitude seemed reflected in a rise of the overall noise level to 62%. This can be seen as a corroboration of the argument that the breaking of the bulk periodicity by a deviation of the position of a substrate atom leads to contributions to the fractional-order intensities that may degrade the simple picture of the adsorbate or adatom as the only path to those fractional-order spots. However, the recovery of a good image, even in this case, clearly suggests that their contribution is small and only serves to increase the background noise level on the image.

These results also help explain the success of our earlier work[9] for the reconstructed SiC(111)-$p(3\times3)$ structure. In that case the application of our algorithm to fractional-order Bragg spot data was able to recover an accurate image of the local site of an adatom despite the fact that other atoms in the surface unit cell were deviated from their positions in an unreconstructed layer.

X. EXPERIMENTAL DATA

As a last step we try to invert experimental data of the O/Ni(001)-$p(2\times2)$ system. After standard crystal preparation, the Ni substrate was subjected to an exposure 2×10^{-8} mbar of O for 60 sec at 90 K. Subsequent annealing at 500 K led to the formation of a sharp $p(2\times2)$ superstructure pattern as evidenced in Fig. 4. The measurement was performed using the standard Video-LEED system developed in Erlangen[4,32] and included four-fold symmetry averaging according to the expected rotational symmetry of the diffraction pattern. The full data set comprises the eight symmetry inequivalent fractional-order beams closest to specular

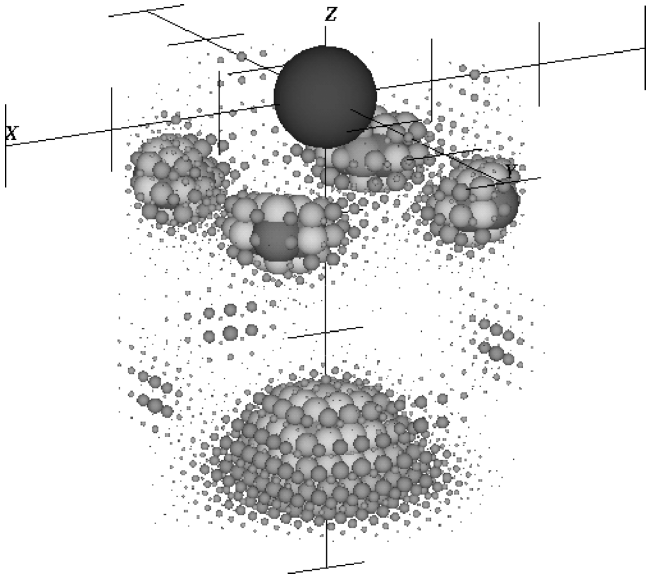

FIG. 5. Same as Fig. 3, except that the image is computed from experimental data from a O/Ni(001)-$p(2\times2)$ surface. The energy range used was 90–344 eV, the kernel constant $C=0.33$ Å and the maximum noise level was 50% of the maxima at the atoms.

reflection in the energy range 90–344 eV. Good agreement of this enlarged data set was found with the three fractional-order spot $I(V)$ curves used in the earlier quantitative LEED study.[29]

Figure 5 shows the reconstructed local adsorption geometry. Although the experimental data set is smaller with respect to the total energy range and the total number of fractional-order beams, we nevertheless find essentially the same stability, accuracy, and unambiguity of the image as described for the other data sets. Even on reducing the number of symmetrically inequivalent beams used to the five nearest to the (00) beam in the diffraction patterns, the image continued to reliably show the four-fold hollow adsorption site with an only slightly degraded overall image quality.

This final result shows, that no particularly large data set needs to be measured to ensure a proper working of the reconstruction algorithm. Rather, it is the same $I(V)$ curves that are measured for a quantitative LEED analysis that also provide the input to the holographic inversion. Ultimately, it is only this similarity of required data that can make holographic LEED a practically useful complement to the established quantitative LEED analysis at the present time.

XI. CONCLUSIONS

We have shown in this paper that a fully three-dimensional image of the adsorption site of atoms forming a $p(2\times2)$ overlayer on a metal surface may be recovered from a data set that might typically be measured in the usual practice of conventional LEED studies, i.e., one from just the most reliably measured normal-incidence LEED data. We have demonstrated this first for a simulated data set from models of O/Ni(001)-$p(2\times2)$ and K/Ni(001)-$p(2\times2)$ surfaces with unreconstructed substrates. The usual picture of holographic LEED from adsorbates on surfaces assumes that the intensities of the fractional-order spots arise only from scattering paths that include a scattering at the adsorbate. This is not strictly true in the presence of substrate reconstructions, which also cause deviations from the periodicity

of the bulk lattice. O/Ni(001)-$p(2\times2)$ is a particularly well-known system with an adsorbate-induced substrate reconstruction. We show that realistic LEED $I(V)$ curves calculated from the accepted model of this substrate reconstruction also give a clear and unambiguous holographic image of the local adsorption site of the O atom. A similar image is also reconstructed from experimental LEED data from this surface.

ACKNOWLEDGMENTS

K.R. is grateful for a DAAD travel grant enabling the stay at the University of Wisconsin-Milwaukee during which this paper was written. The Milwaukee group acknowledges support from the U.S. NSF (Grant No. DMR-9320275) and the Erlangen authors support by the German DFG.

*On leave from: Lehrstuhl für Festkörperphysik, Universität Erlangen-Nürnberg, Germany.

[1] J. B. Pendry, *Low Energy Electron Diffraction* (Academic, London, 1974); M. A. van Hove, W. H. Weinberg, and C.-M. Chan, *Low Energy Electron Diffraction* (Springer-Verlag, Berlin, 1986).

[2] M. A. van Hove and S. Y. Tong, *Surface Crystallography by LEED* (Springer-Verlag, Berlin, 1979).

[3] M. A. van Hove, W. Moritz, H. Over, P. J. Rous, A. Wander, A. Barbieri, N. Materer, U. Starke, and G. A. Somorjai, Surf. Sci. Rep. **19**, 191 (1993).

[4] K. Heinz, Rep. Prog. Phys. **58**, 637 (1995).

[5] P. J. Rous, Surf. Sci. **296**, 358 (1993); R. Döll and M. A. van Hove, *ibid.* **355**, L393 (1996); M. Kottcke and K. Heinz, *ibid.* **376**, 352 (1997).

[6] J. B. Pendry, K. Heinz, and W. Oed, Phys. Rev. Lett. **61**, 2953 (1988); J. B. Pendry and K. Heinz, Surf. Sci. **230**, 137 (1990).

[7] A. Szöke, in *Short Wavelength Coherent Radiation: Generation and Applications*, edited by D. J. Attwood and J. Boker, AIP Conf. Proc. No. 147 (AIP, New York, 1986).

[8] D. K. Saldin and P. L. De Andres, Phys. Rev. Lett. **64**, 1270 (1990).

[9] K. Reuter, J. Bernhardt, H. Wedler, J. Schardt, U. Starke, and K. Heinz, Phys. Rev. Lett. **79**, 4818 (1997).

[10] K. Heinz, U. Starke, and F. Bothe, Surf. Sci. Lett. **243**, L70 (1991); K. Heinz, U. Starke, M. A. van Hove, and G. A. Somorjai, Surf. Sci. **261**, 57 (1992).

[11] M. A. Mendez, C. Glück, and K. Heinz, J. Phys.: Condens. Matter **4**, 999 (1992); M. A. Mendez, C. Glück, M. Wagner, U. Löffler, R. Döll, and K. Heinz, Surf. Sci. **290**, 45 (1993).

[12] P. Hu and D. A. King, Nature (London) **360**, 656 (1992).

[13] S. Y. Tong, H. Huang, and X. Q. Guo, Phys. Rev. Lett. **69**, 3654 (1992).

[14] C.-M. Wei, S. Y. Tong, H. Wedler, M. A. Mendez, and K. Heinz, Phys. Rev. Lett. **72**, 2434 (1994).

[15] K. Heinz and H. Wedler, Surf. Rev. Lett. **1**, 319 (1994).

[16] D. K. Saldin, K. Reuter, P. L. de Andres, H. Wedler, X. Chen, J. B. Pendry, and K. Heinz, Phys. Rev. B **54**, 8172 (1996).

[17] D. K. Saldin, X. Chen, J. A. Vamvakas, M. Ott, H. Wedler, K. Reuter, and K. Heinz, Surf. Rev. Lett. **4**, 991 (1997).

[18] J. B. Pendry and D. K. Saldin, Surf. Sci. **145**, 33 (1984).

[19] J. J. Barton, Phys. Rev. Lett. **61**, 1356 (1988).

[20] J. J. Barton, Phys. Rev. Lett. **67**, 3106 (1991).

[21] K. Heinz, R. Döll, M. Wagner, U. Löffler, and M. A. Mendez, Appl. Surf. Sci. **70/71**, 367 (1993).

[22] S. Y. Tong, Hua Li, and H. Huang, Phys. Rev. Lett. **67**, 3102 (1991).

[23] D. K. Saldin, Surf. Rev. Lett. **4**, 441 (1997).

[24] D. K. Saldin and X. Chen, Phys. Rev. B **52**, 2941 (1995).

[25] C.-M. Wei and S. Y. Tong, Surf. Sci. **274**, L577 (1992).

[26] K. Reuter, H. Wedler, M. Ott, K. Heinz, J. A. Vamvakas, X. Chen, and D. K. Saldin, Phys. Rev. B **55**, 5344 (1997).

[27] W. H. Press, S. A. Teukolsky, W. T. Vetterling, and B. P. Flannery, *Numerical Recipes* (Cambridge University Press, Cambridge, 1986).

[28] Note that Ref. 27 defines Fourier transforms with the factor 2π separate from the frequency in the phase factor. This factor hence does not appear in their formulation of the sampling theorem.

[29] W. Oed, H. Lindner, U. Starke, K. Heinz, K. Müller, D. K. Saldin, P. L. de Andres, and J. B. Pendry, Surf. Sci. **225**, 242 (1990).

[30] H. Wedler, M. A. Mendez, P. Bayer, U. Löffler, K. Heinz, V. Fritsche, and J. B. Pendry, Surf. Sci. **293**, 47 (1993).

[31] The depth of the reconstructed real-space volume was for this calculation increased to 5.0 Å to include the second-layer atom.

[32] K. Müller and K. Heinz, Surf. Sci. **2**, 105 (1985).